

The object of this study is the background substrate of astronomical frames. To detect and compare the image of an object in a frame with its real image from astronomical catalogs, it is necessary to uniformly distribute the brightness of the background image substrate. Most often, the background alignment of astronomical frames is performed using the hardware calibration method applying the construction of service frames. However, it does not make it possible to eliminate the background from temporary stray light. Therefore, to solve this problem, a procedure has been proposed for brightness alignment of the background frame using high-pass filtering.

For high-pass filtering of images, three high-pass filters were considered – an ideal filter, a Butterworth filter, and a Gaussian filter. To remove coarse-grained image components from the image, a high-pass filter was used, which attenuates low-frequency harmonics of the image spectrum while simultaneously passing high-frequency harmonics.

Applying the devised procedure for brightness alignment of the background substrate of the frame has made it possible to increase the signal-to-noise ratio and reduce the dynamic range of the background substrate of the image. The study showed that when assessing brightness and identifying frames, the fitting provides better accuracy of reference to the starry sky. Also, the standard deviation of frame identification errors in this case is 5–7 times less than without using the devised procedure.

The devised procedure for brightness alignment of the background frame substrate was tested in practice within the framework of the CoLiTec project. It was implemented at the stage of intra-frame processing in the Lemur software for automated detection of new objects and tracking of known objects

Keywords: brightness equalization, high-pass filtering, ideal filter, Butterworth filter, Gaussian filter

DEVISING A PROCEDURE FOR THE BRIGHTNESS ALIGNMENT OF ASTRONOMICAL FRAMES BACKGROUND BY A HIGH FREQUENCY FILTRATION TO IMPROVE ACCURACY OF THE BRIGHTNESS ESTIMATION OF OBJECTS

Vladimir Vlasenko
PhD

Space Research and Communications Center
National Space Facilities Control and Test Center
Moskovska str., 8, Kyiv, Ukraine, 01010

Sergii Khlamov
Corresponding author

PhD, Assistant

Department of Media Systems and Technologies*

E-mail: sergii.khlamov@gmail.com

Vadym Savanevych

Doctor of Technical Sciences, Professor

Department of Systems Engineering*

*Kharkiv National University of Radio Electronics

Nauky ave., 14, Kharkiv, Ukraine, 61166

Received date 09.02.2024

Accepted date 15.04.2024

Published date 30.04.2024

How to Cite: Vlasenko, V., Khlamov, S., Savanevych, V. (2024). Devising a procedure for the brightness alignment of astronomical frames background by a high frequency filtration to improve accuracy of the brightness estimation of objects. *East-European Journal of Enterprise Technologies*, 2 (2 (128)), 31–38. <https://doi.org/10.15587/1729-4061.2024.301327>

1. Introduction

The global community is constantly faced with issues related to potential asteroid-comet hazard [1]. To prevent this threat, there is an area of observational astronomy, which not only receives and accumulates astronomical frames but also processes the resulting images. This area continues to actively evolve due to the constant improvement of various methods of astrometry [2] and photometry [3]. Owing to improvements and breakthroughs in digital technologies, as well as telescope construction, it has become possible to accumulate large amounts of data [4]. These raw astronomical data are received as results from asteroid/comet/satellite surveys for subsequent automated processing. During such processing, huge astronomical catalogs and archival big data are also involved [5]. This is making it possible to

accumulate, obtain knowledge [6] and analyze accumulated publicly available data [7] and measurements. Basically, they were acquired over a long period of observation of specific celestial objects of the Solar System (SSO) [8] (for example, asteroids [9] or comets), as well as artificial satellites [10]. This analysis may also include calculation of the period and shape of rotations of such SSOs [11].

When carrying out photometric measurements on a series of digital frames, strict requirements are put forward for the uniform distribution of the brightness of the background component of the image over the entire digital frame. This is necessary for a more accurate comparison of a specific image of a potential SSO with its real image from astronomical catalogs during the frame identification procedure. Traditionally, background alignment of astronomical frames is performed using hardware

calibration. However, this approach is very resource- and time-consuming and is a labor-intensive and inconvenient operation for the observer.

Therefore, it is relevant task to devise a procedure for brightness alignment of the background substrate of a frame. This procedure will increase the signal-to-noise ratio (SNR) and reduce the dynamic range of the background image. This in turn will minimize the number of false measurements and speed up the identification process. This will also make it possible to more accurately estimate the brightness and positional coordinates of the objects under study [12], which will increase the conditional probability of correct detection (CPCD) of real objects [13].

2. Literature review and problem statement

In general, SSO images on digital frames are formed using a charge-coupled device (CCD) [14].

The uniformity of the standard image shape of objects [15] is an important factor influencing the subsequent process of brightness assessment and identification with the astronomical catalog. Therefore, it is necessary to conduct an in-depth analysis of literature data to compare methods for preparing images for the identification process itself. Such methods are expected to reduce the shift in the positional coordinates of the frame center between the frames themselves in the series.

For example, classical methods of computer vision [16] and object image recognition [17] are not able to provide the required level of processing speed. These methods require the analysis of all pixels of potential objects to determine their typical shape. However, when the standard form is heterogeneous, objects become confused, which increases the processing and identification time. Methods for estimating image parameters [18, 19] are based on the analysis of only those pixels that potentially belong to the object under study. Their disadvantage is the inability to initially accurately determine specific pixels and reject those whose intensity exceeds a specified limit value.

In study [20], the authors use automatic selection of a reference point to select calibration frames. However, this is not a requirement for the identification process itself because if there are artifacts in the image, these control points may be false. Thus, the accuracy of identification with real objects from the astronomical catalog decreases.

Another method for obtaining frames for pre-calibration involves combining a large number of frames to get rid of real objects, leaving only a uniform background signal. This method is termed the median pooling algorithm [21]. However, to create good digital images with a high signal-to-noise ratio using this method requires a lot of images. This also leads to the loss of real objects at a specific time of their observation.

In [22], a segmentation method is proposed. However, it only works with single images of objects. That is, in the case of a variety of standard shapes (strokes, extended, circular) or the intersection of an object image with light flare, this method will not provide the necessary accuracy due to the ambiguity of the number of brightness peaks.

This variety of typical shapes also influences various methods for cluster analysis of large data sets [4], Wavelet transform [23], and time series analysis [24]. The disadvan-

tage of these methods is that they can only work with “pure” measurements, so the heterogeneity of the images will greatly spoil the overall indicator.

Another implementation is reported in study [25] in the form of an additional calibration procedure to avoid the internal coma of the telescope’s secondary mirror. But, to equalize brightness and remove “highlights”, there is a brightness method that is more improved in accuracy and quality using an inverse median filter [26]. However, the disadvantage of these implementations is the poor accuracy of positional coordinate estimates during the identification process itself between frames of the same series.

The matched filtering procedure is also known [27, 28], but it uses only an analytical image model. The disadvantage of this procedure is the inaccuracy of identification when the typical image of an object is different in different frames of the series. The classical method of adding frames [29, 30] to improve the “super” frame is also ineffective in the case when the SSO image does not have clear boundaries on all digital frames of the series.

Based on the above, most existing processing methods for detecting single images of objects require instrumental calibrations. This is necessary to prepare more “clean” frames for using already known detection methods. However, in the case where there is no possibility of generating fresh calibration frames or the presence of already generated archive frames, these methods demonstrate poor accuracy in estimating image parameters. Therefore, it is necessary to devise a procedure for brightness alignment of the background frame, which will take into account the peculiarities of frame formation and will make it possible to prepare a “clean” frame for subsequent processing.

3. The aim and objectives of the study

The purpose of our study is to devise a procedure for brightness alignment of the background frame to improve the accuracy of object detection. This will make it possible to increase the SNR and reduce the dynamic range of the background image.

To achieve the goal, the following tasks were set:

- to determine the transfer characteristic of the high-frequency filter;
- to develop an algorithm for the procedure for brightness alignment of the background frame;
- to verify the procedure for brightness alignment of the background frame.

4. The study materials and methods

The object of our study is SSO images on a series of digital frames. The initial series for the study were obtained from a variety of telescopes installed at observatories in Ukraine and around the world. Namely, the ISON-NM observatory, the SANTEL-400AN telescope (New Mexico, USA); Vihorlat Observatory, VNT telescope (Humenne, Slovakia) [26]; Odesa-Mayaky Observatory, OMT-800 telescope (Mayaki, Ukraine) [31]; Cerro Tololo observatory, PROMPT-8 telescope (La Serena, Chile) [32].

The work puts forward a working hypothesis assuming that when performing high-frequency filtering of the back-

ground substrate of the frame, the accuracy of detecting objects in the frame will increase.

The assumption accepted is that in order to improve accuracy, the signal-to-noise ratio will be increased in all considered object images. The dynamic range of the image's background will also be reduced. The work also put forward a simplification, which is associated with the uniformity of the standard form of images of all objects in the frame and the absence of their synchronous blur.

The USNO B1.0 catalog [33] was used as an astronomical catalog. The catalog contains angular positional coordinates and magnitude of more than one billion SSOs, formed over 3.6 billion measurements.

The methods used for the study were high-pass filtering methods, namely ideal filter, Butterworth filter, and Gaussian filter.

The accuracy of brightness estimation and object detection deteriorates significantly with a certain feature of the formation of astronomical frames – vignetting. This is a gradual decrease in image brightness from the center to the edges of the field of view of the optical system, which reduces the SNR of object images (Fig. 1).

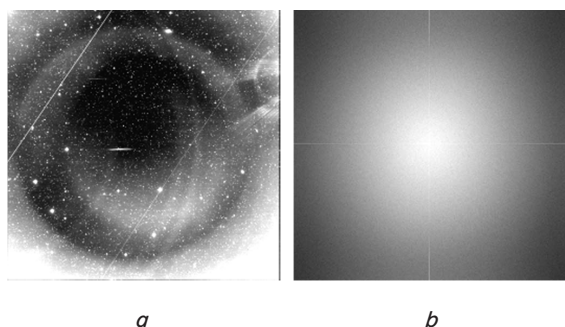


Fig. 1. Astronomical image: *a* – original image with light flare; *b* – light flare spectrum module

Digital images on astronomical frames are divided into coarse-grained and fine-grained components. Each of these components has its own physical nature of origin.

The coarse-grained component of the images corresponds to image illumination during astronomical observations during the full moon or at sunrise and sunset and occupies significant parts of the frames (Fig. 2, *a*).

The fine-structure components correspond to the SSO images (Fig. 2, *b*). The size of fine-grained components of images usually takes 5÷10 pixels and does not exceed 50÷60 pixels.

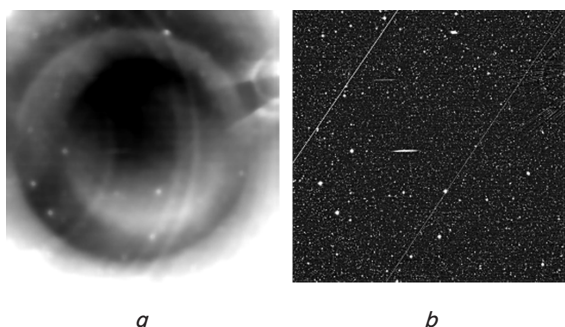


Fig. 2. Astronomical image: *a* – coarse-grained component; *b* – fine-structured component

Another feature of the formation of astronomical frames that must be taken into account is the influence of the telescope control system in conjunction with the rotating support device. Violation of the telescope's clock control is the main reason for blurred images of objects in the astronomical frame. This also leads to a shift in the equatorial coordinates of the frame centers.

The difference in the spectrum of the SSO images and the background substrate of the frame makes it possible to use frequency filtering of the image. The result of this is an increase in SNR and a decrease in the dynamic range of the background image. To remove large-structure components from an image, it is advisable to use a high-frequency filter, which attenuates low-frequency harmonics of the image spectrum while simultaneously transmitting high-frequency harmonics.

Our research results, as well as the devised procedure for brightness alignment of the background frame, were implemented in the C++ programming language. This code was implemented at the stage of intra-frame processing of the Lemur software package (Ukraine) [34] for the automated detection of new and maintenance of known objects within the CoLiTec project [35].

The devised procedure, implemented in Lemur software (Ukraine), was used during the successful identification of digital frames, which contained a total of more than 800,000 SSOs. Their measurements were also successfully identified with known astronomical catalogs. This fact confirmed the practical importance of the procedure for brightness leveling of the background substrate of the frame.

5. Results of investigating the procedure for brightness alignment of the background substrate of the frame

5.1. Determining the transfer characteristic of a high-frequency filter

By filtering astronomical frames, the high-frequency component of the image can be emphasized. This is possible owing to high-pass filtering of images. It can be implemented in the spatial and frequency domains [36]. In the frequency domain, the high-pass filtering operation is equivalent to the product of the image spectrum and the transfer function of the high-pass filter. The filter's transfer function specifies a multiplier for each harmonic of the image spectrum. The corresponding harmonic of the image spectrum is multiplied by this factor. In this case, the transfer function of the high-frequency filter suppresses the frequencies of the image spectrum that lie in the region, the Euclidean distance from which to the center of the spectrum is limited by the cutoff frequency ω_0 [37].

In the spatial domain, high-pass image filtering is implemented as the operation of convoluting an image with the impulse response of a high-pass filter [29]. The impulse response of a high-pass filter is the response of the filter to a two-dimensional unit pulse $\delta(m, n)$, which is given by:

$$\delta(m, n) = \begin{cases} 1, & \text{at } m = n = 0, \\ 0, & \text{at } m \neq n, \end{cases} \quad (1)$$

where m, n are pixel numbers.

The impulse response of a high-pass filter is equal to the inverse discrete Fourier transform of the transfer function of the high-pass filter [36]. Therefore, it is necessary to select

the transfer function of a high-frequency filter that would satisfy the peculiarities of the formation of astronomical frames. The most commonly used high-pass filters for various purposes are the ideal filter, the Butterworth filter, and the Gaussian filter.

The transfer function $H_{Ihp}(u, v)$ of an ideal high-pass filter is described by the following expression:

$$H_{Ihp}(u, v) = \begin{cases} 0, & \text{at } r(u, v) \leq \omega_0, \\ 1, & \text{at } r(u, v) > \omega_0, \end{cases} \quad (2)$$

where u, v – numbers of frequency components of the spectrum

$r(u, v) = 2\pi\sqrt{(u - E[N/2])^2 / N^2 + (v - E[M/2])^2 / M^2}$ – distance from the point (u, v) of the frequency domain to the origin of the spectrum;

$M \times N$ – the size of the filter transfer function, equal to the size of the image spectrum over which high-frequency filtering is carried out;

$E[\bullet]$ – operation of taking the integer part of a number.

An ideal high-pass filter nulls the spectral components of an image with frequencies that fall within a region centered at the beginning of the frequency domain and radius ω_0 and passes spectral components that lie outside this region. The transfer function of an ideal high-pass filter with its perspective and grayscale images is represented below (Fig. 3).

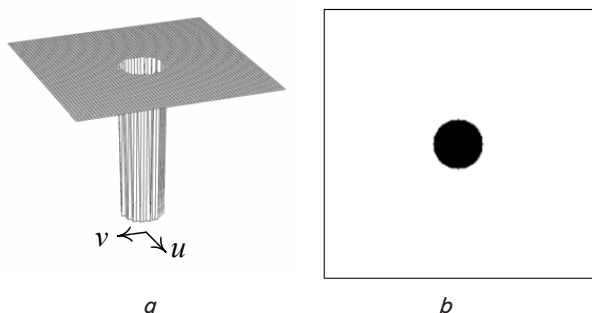


Fig. 3. Transfer function of a high-frequency ideal filter: *a* – perspective image; *b* – half-tone image

The transfer function $H_{Bhp}(u, v)$ of a high-pass Butterworth filter of order p is described by the following expression:

$$H_{Bhp}(u, v) = \frac{1}{1 + [\omega_0 / r(u, v)]^{2p}}. \quad (3)$$

For a high-frequency Butterworth filter, the cutoff frequency ω_0 determines the region in which the frequency components of the image spectrum are reduced by a factor of 2 or more. The transfer function of the high-pass Butterworth filter with its perspective and grayscale images is represented below (Fig. 4).

The transfer function $H_{Ghp}(u, v)$ of the high-pass Gaussian filter is described by the following expression:

$$H_{Ghp}(u, v) = 1 - \exp\left(-\frac{r^2(u, v)}{2\sigma_\omega^2}\right), \quad (4)$$

where σ_ω is the shape parameter of the transfer function of the high-frequency Gaussian filter.

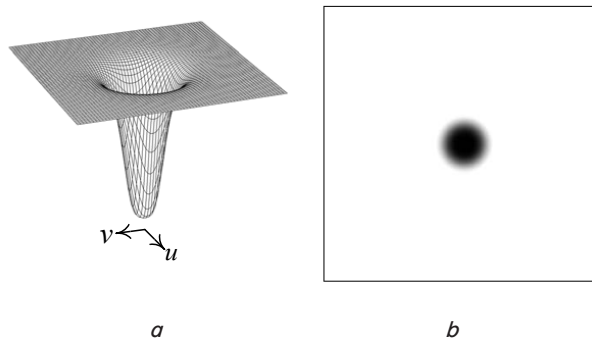


Fig. 4. Transfer function of the high-frequency Butterworth filter: *a* – perspective image; *b* – half-tone image

The transfer function of the high-pass Gaussian filter suppresses frequency components lying in the region limited by the radius σ_ω . In this case, the harmonics of the image spectrum with frequencies equal to the cutoff frequency of the Gaussian filter itself $\omega_0 = \sigma_\omega$ are suppressed by 2.5 times. The transfer function of the high-pass Gaussian filter with its perspective and grayscale images is represented below (Fig. 5).

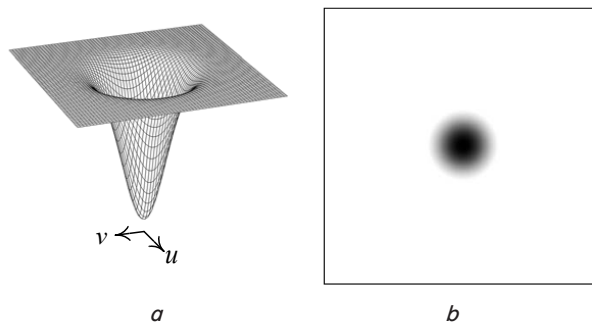


Fig. 5. Transfer function of a high-frequency Gaussian filter: *a* – perspective image; *b* – half-tone image

In this work, a high-frequency Gaussian filter is determined through the length of its impulse response $M_{hx} = M_{hy} = M_h$.

5. 2. Development of an algorithm for the procedure for brightness alignment of the background frame

The algorithm for the procedure for brightness leveling the background of a frame using high-pass filtering includes the following sequence of operations:

1. Formation of a set Θ_{bg} of pixels of the background of the entire digital frame.
2. Formation of a discrete spectrum of the original image S_{in} using the direct discrete Fourier transform of the original image A_{in} :

$$S_{in}(u, v) = \sum_{m=0}^{N_{CCDx}-1} \sum_{n=0}^{N_{CCDy}-1} A_{in}(m, n) \exp\left(\begin{matrix} -i \frac{2\pi}{N_{CCDx}} mu - \\ -i \frac{2\pi}{N_{CCDy}} nv \end{matrix} \right), \quad (5)$$

where $S_{in}(u, v)$ is the uv -th harmonic of the discrete spectrum of the original image;

$A_{in}(m, n)$ – brightness of the mn -th pixel of the original image.

3. Determination of the transfer function H_{Ghp} of the high-pass filter that will be used during the study, for example a Gaussian filter (4).

4. Formation of the spectrum of the high-frequency component of the original image S_{hp} by multiplying the spectrum of the original image S_{in} and the transfer function H_{Ghp} :

$$S_{hp}(u,v) = S_{in}(u,v)H_{Ghp}(u,v), \quad (6)$$

where $S_{hp}(u,v)$ is the uv -th harmonic of the spectrum of the high-frequency component of the original image.

5. Determination of the high-frequency component of the original image A_{hp} as the inverse discrete Fourier transform of its spectrum:

$$A_{hp}(m,n) = \sum_{u=0}^{N_{CCDx}-1} \sum_{v=0}^{N_{CCDy}-1} S_{hp}(u,v) \exp \left(i \frac{2\pi}{N_{CCDx}} mu + i \frac{2\pi}{N_{CCDy}} nv \right) \quad (7)$$

where $A_{hp}(m,n)$ is the brightness of the mn -th pixel of the high-frequency component of the original image.

6. Final removal of coarse-grained image components from the original image itself using the resulting high-frequency component of the original image (7).

5.3. Verification of the procedure for brightness alignment of the background frame

To verify the devised procedure for brightness alignment of the background frame using high-frequency filtering, testing was carried out on a series of frames obtained from various telescopes. The frames were selected in such a way that they contained light flare, distortions, and image artifacts. The devised procedure for brightness alignment of the background frame was tested using the following high-pass filters: ideal, Butterworth, and Gaussian. The processing results are shown below in Fig. 6.

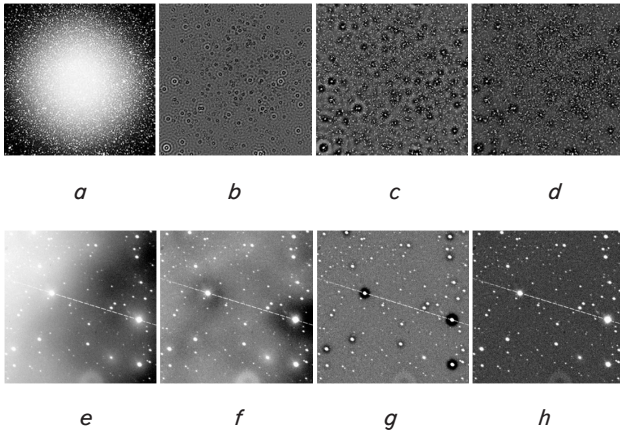


Fig. 6. Result of high-frequency filtering of the image:
a, e – original image; *b, f* – ideal filter;
c, g – Butterworth filter; *d, h* – Gaussian filter

The main indicator of the quality of luminance equalization is the global SNR in the digital frame. It is calculated as the ratio of the average brightness of the set of pixels belonging to the image of the k -th object to the standard deviation of the background brightness on the set of back-

ground pixels of the entire digital frame. For clarity of the difference between high-frequency filters, Table 1 gives the values of the residual dispersion of the difference between the local SNR on the original and filtered frames for the three high-frequency filters under consideration. The chosen equal frequency for all filters was $D=6.9$; the order $p=5$ was chosen for the Butterworth filter.

Table 1

Values of the residual variance of the difference between the local SNR on the original and filtered frames

High Pass Filter	Value
Ideal filter	4.0816
Butterworth filter	4.3157
Gaussian filter	3.6628

Based on the values of the residual variance of the difference between the local SNR on the original and filtered frames, the Gaussian filter with the lowest value was selected for further research. Analysis of the global SNR and its comparison with the local SNR for the Gaussian filter is shown in Fig. 7. Local and global SNR of object images were calculated for one frame. The considered parameters were obtained for 3500 images of objects in the frame. In Fig. 7, the abscissa axis shows the parameters (pixel brightness value in grayscale from 0 to 255), calculated on the original frame, and the ordinate – on the frame after filtering.

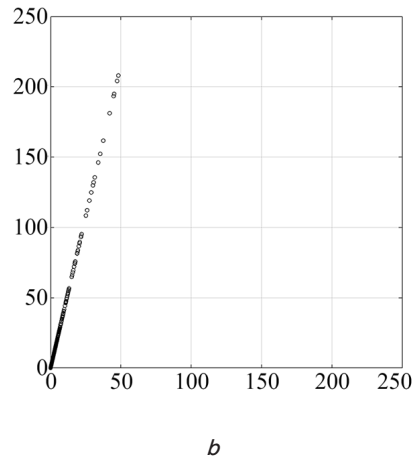
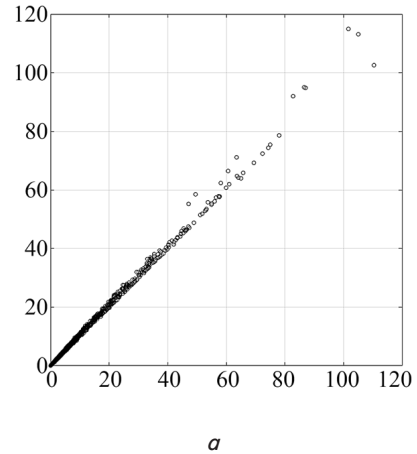


Fig. 7. Quality indicators: *a* – local signal-to-noise ratio; *b* – global signal-to-noise ratio

The results of the study shown in Fig. 7 indicate successful verification of the devised procedure and confirmation of the working hypothesis put forward. Performing high-frequency filtering of the background of the frame allows one to increase the accuracy of detecting objects in the frame. This is due to the fact that the global SNR after background leveling increases by more than 5 times in all considered images of objects.

6. Discussion of results of investigating the procedure for brightness alignment of the background frame

A study was conducted into the procedure for brightness alignment of the background frame using high-frequency filtering. The features of the formation of series of digital images of objects on astronomical frames were analyzed. The following were chosen as high-frequency filters: ideal (2), Butterworth (3), and Gaussian (4). Each of these filters was used in the devised procedure and was analyzed.

The impulse response of an ideal high-pass filter has a two-dimensional unit impulse at the center and circular concentric components located around it. Experimental studies have revealed that when astronomical images are filtered with this filter, a so-called “ringing” appears, which significantly worsens the assessment of the brightness of objects. With increasing order, the transfer function of the Butterworth high-pass filter (3) approaches the transfer function of an ideal high-pass filter. Also, with increasing order, the impulse response acquires similar properties to the impulse response of an ideal high-frequency filter. Only with the first order high-pass Butterworth filter, the filtering result does not have ringing artifacts. The transfer function of the high-pass Gaussian filter (4) depends on the parameters of the Gaussian function used. The discrete Fourier transform of a Gaussian function is also a Gaussian function [36]. Therefore, the impulse response does not have concentric rings. Therefore, the resulting images after filtering with a Gaussian filter are also free of “ringing” artifacts.

As part of the CoLiTec project, research was carried out into the application of the devised procedure for brightness alignment of the background frame substrate using high-frequency filtering (Fig. 6). After the analysis, the Gaussian filter was chosen as a high-pass filter for the procedure, which showed the best results in terms of SNR (Fig. 7). This result is determined by the selected transfer function of this filter since the absence of concentric rings and ringing artifacts increases the SNR.

The study showed that the use of the devised procedure reduces identification errors with cataloged (reference) objects by 5–7 times [18]. Statistical modeling [38] has proven that this significantly affects the quality and accuracy of a number of data acquisition and retrieval tasks [39]. This also affects brightness estimation and detection of object trajectories [40, 41] using supercomputers [42].

The limitation of our study is the size of the generated CCD frames, as well as the uniform shooting conditions for each frame of the series. The type of CCD matrix affects the angular size and field of view, which leads to a varied number of SSOs in frames (from hundreds to tens of thousands). Another limitation is the computing power of the equipment on which the processing will take place. The issue of security [43] of frames, namely the encryption of input data, is also important. In this case, an additional decryption algorithm will be required.

The disadvantage of the study is that when implementing the proposed procedure, it is necessary to first analyze the artifacts of the astronomical image. This is required for a more correct selection of the transfer function of the high-frequency filter for use in the procedure.

It is advisable to focus further research on the simultaneous application of the devised procedure and calibration by service frames [25]. This will be necessary to accumulate and obtain data [44] for further brightness assessment and identification of SSO with astronomical catalogs. To this end, it will be necessary to design a processing pipeline, connections to astronomical catalogs, and corresponding methods for retrieving services/modules [45]. It is also necessary to evaluate the usefulness of the devised procedure for other mathematical models [46], as well as methods for recognizing objects and detecting their movement, which will be used subsequently. To do this, one can use machine learning, Wavelet analysis [47], time series analysis or forecasting method [48] to calculate indicators. The task of further research is to apply the devised procedure as a stage of preliminary image preparation before applying basic image processing methods.

7. Conclusions

1. The transfer characteristic of the high-frequency filter was determined. The following high-pass filters were chosen: ideal, Butterworth, and Gaussian. Each of these filters was used in the devised procedure and was analyzed. Our analysis revealed that with increasing order, the transfer function of the Butterworth filter approaches the transfer function of an ideal filter. And from this it follows that both filters result in concentric rings and, as a result, “ringing” type artifacts.

2. An algorithm was developed for the procedure for brightness alignment of the background frame using high-frequency filtering. The key point is the formation of the spectrum of the high-frequency component of the original image based on the selected transfer function. The Gaussian transfer function was chosen as it. A feature of this function is the absence of concentric rings in the spectrum and smoothed brightness transitions. This made it possible to determine the high-frequency component of the original image, which can subsequently be removed as a coarse-grained component of the image.

3. The devised procedure for brightness alignment of the background frame using high-frequency filtering was verified based on many series of frames containing at least 3500 objects. The application of the devised procedure increases the signal-to-noise ratio by more than 5 times in all considered images of objects and reduces the dynamic range of the background image substrate by more than 3 times.

Conflicts of interest

The authors declare that they have no conflicts of interest in relation to the current study, including financial, personal, authorship, or any other, that could affect the study and the results reported in this paper.

Funding

The study was conducted without financial support.

Data availability

All data are available in the main text of the manuscript.

Use of artificial intelligence

The authors confirm that they did not use artificial intelligence technologies when creating the current work.

References

1. Wheeler, L., Dotson, J., Aftosmis, M., Coates, A., Chomette, G., Mathias, D. (2024). Risk assessment for asteroid impact threat scenarios. *Acta Astronautica*, 216, 468–487. <https://doi.org/10.1016/j.actaastro.2023.12.049>
2. Khlamov, S. V., Savanevych, V. E., Briukhovetskiy, O. B., Pohorelov, A. V. (2016). CoLiTec software - detection of the near-zero apparent motion. *Proceedings of the International Astronomical Union*, 12 (S325), 349–352. <https://doi.org/10.1017/s1743921316012539>
3. Savanevych, V. E., Khlamov, S. V., Akhmetov, V. S., Briukhovetskiy, A. B., Vlasenko, V. P., Dikov, E. N. et al. (2022). CoLiTecVS software for the automated reduction of photometric observations in CCD-frames. *Astronomy and Computing*, 40, 100605. <https://doi.org/10.1016/j.ascom.2022.100605>
4. Hu, Z., Bodyanskiy, Y. V., Tyshchenko, O. K., Tkachov, V. M. (2017). Fuzzy Clustering Data Arrays with Omitted Observations. *International Journal of Intelligent Systems and Applications*, 9 (6), 24–32. <https://doi.org/10.5815/ijisa.2017.06.03>
5. Vavilova, I., Pakuliak, L., Babyk, I., Elyiv, A., Dobrycheva, D., Melnyk, O. (2020). Surveys, Catalogues, Databases, and Archives of Astronomical Data. *Knowledge Discovery in Big Data from Astronomy and Earth Observation*, 57–102. <https://doi.org/10.1016/b978-0-12-819154-5.00015-1>
6. Zhang, Y., Zhao, Y., Cui, C. (2002). Data mining and knowledge discovery in database of astronomy. *Progress in Astronomy*, 20 (4), 312–323.
7. Chalvi, S., Levykin, I., Biziuk, A., Vovk, A., Bogatov, I. (2020). Development of the technology for changing the sequence of access to shared resources of business processes for process management support. *Eastern-European Journal of Enterprise Technologies*, 2 (3 (104)), 22–29. <https://doi.org/10.15587/1729-4061.2020.198527>
8. Khlamov, S., Savanevych, V., Tabakova, I., Trunova, T. (2022). The astronomical object recognition and its near-zero motion detection in series of images by in situ modeling. 2022 29th International Conference on Systems, Signals and Image Processing (IWSSIP). <https://doi.org/10.1109/iwssip55020.2022.9854475>
9. Troianskiy, V., Kankiewicz, P., Oszkiewicz, D. (2023). Dynamical evolution of basaltic asteroids outside the Vesta family in the inner main belt. *Astronomy & Astrophysics*, 672, A97. <https://doi.org/10.1051/0004-6361/202245678>
10. Akhmetov, V., Khlamov, S., Savanevych, V., Dikov, E. (2019). Cloud Computing Analysis of Indian ASAT Test on March 27, 2019. 2019 IEEE International Scientific-Practical Conference Problems of Infocommunications, Science and Technology (PIC S&T). <https://doi.org/10.1109/picst47496.2019.9061243>
11. Oszkiewicz, D., Troianskiy, V., Galád, A., Hanuš, J., Ďurech, J., Wilawer, E. et al. (2023). Spins and shapes of basaltic asteroids and the missing mantle problem. *Icarus*, 397, 115520. <https://doi.org/10.1016/j.icarus.2023.115520>
12. Savanevych, V., Khlamov, S., Briukhovetskiy, O., Trunova, T., Tabakova, I. (2023). Mathematical Methods for an Accurate Navigation of the Robotic Telescopes. *Mathematics*, 11 (10), 2246. <https://doi.org/10.3390/math11102246>
13. Bellanger, M. (2024). *Digital Signal Processing*. John Wiley & Sons. <https://doi.org/10.1002/9781394182695>
14. Adam, G. K., Kontaxis, P. A., Doulos, L. T., Madias, E.-N. D., Bouroussis, C. A., Topalis, F. V. (2019). Embedded Microcontroller with a CCD Camera as a Digital Lighting Control System. *Electronics*, 8 (1), 33. <https://doi.org/10.3390/electronics8010033>
15. Savanevych, V., Khlamov, S., Vlasenko, V., Deineko, Z., Briukhovetskiy, O., Tabakova, I., Trunova, T. (2022). Formation of a typical form of an object image in a series of digital frames. *Eastern-European Journal of Enterprise Technologies*, 6 (2 (120)), 51–59. <https://doi.org/10.15587/1729-4061.2022.266988>
16. Klette, R. (2014). *Concise Computer Vision. An Introduction into Theory and Algorithms*. Springer London, 429. <https://doi.org/10.1007/978-1-4471-6320-6>
17. Khlamov, S., Tabakova, I., Trunova, T. (2022). Recognition of the astronomical images using the Sobel filter. 2022 29th International Conference on Systems, Signals and Image Processing (IWSSIP). <https://doi.org/10.1109/iwssip55020.2022.9854425>
18. Dhanalakshmi, R., Bhavani, N. P. G., Raju, S. S., Shaker Reddy, P. C., Mavaluru, D., Singh, D. P., Batu, A. (2022). Onboard Pointing Error Detection and Estimation of Observation Satellite Data Using Extended Kalman Filter. *Computational Intelligence and Neuroscience*, 2022, 1–8. <https://doi.org/10.1155/2022/4340897>
19. Savanevych, V., Akhmetov, V., Khlamov, S., Dikov, E., Briukhovetskiy, A., Vlasenko, V. et al. (2019). Selection of the Reference Stars for Astrometric Reduction of CCD-Frames. *Advances in Intelligent Systems and Computing*, 881–895. https://doi.org/10.1007/978-3-030-33695-0_57
20. Lösler, M., Eschelbach, C., Riepl, S. (2018). A modified approach for automated reference point determination of SLR and VLBI telescopes. *Tm - Technisches Messen*, 85 (10), 616–626. <https://doi.org/10.1515/teme-2018-0053>
21. Shan, W., Yi, Y., Qiu, J., Yin, A. (2019). Robust Median Filtering Forensics Using Image Deblocking and Filtered Residual Fusion. *IEEE Access*, 7, 17174–17183. <https://doi.org/10.1109/access.2019.2894981>
22. Minaee, S., Boykov, Y. Y., Porikli, F., Plaza, A. J., Kehtarnavaz, N., Terzopoulos, D. (2021). Image Segmentation Using Deep Learning: A Survey. *IEEE Transactions on Pattern Analysis and Machine Intelligence*, 1–1. <https://doi.org/10.1109/tpami.2021.3059968>

23. Dadkhah, M., Lyashenko, V. V., Deineko, Z. V., Shamshirband, S., Jazi, M. D. (2019). Methodology of wavelet analysis in research of dynamics of phishing attacks. *International Journal of Advanced Intelligence Paradigms*, 12 (3/4), 220. <https://doi.org/10.1504/ijaip.2019.098561>
24. Kirichenko, L., Saif, A., Radivilova, T. (2020). Generalized Approach to Analysis of Multifractal Properties from Short Time Series. *International Journal of Advanced Computer Science and Applications*, 11 (5). <https://doi.org/10.14569/ijacsa.2020.0110527>
25. Hampson, K. M., Gooding, D., Cole, R., Booth, M. J. (2019). High precision automated alignment procedure for two-mirror telescopes. *Applied Optics*, 58 (27), 7388. <https://doi.org/10.1364/ao.58.007388>
26. Kudzej, I., Savanevych, V. E., Briukhovetskiy, O. B., Khlamov, S. V., Pohorelov, A. V., Vlasenko, V. P. et al. (2019). CoLiTecVS – A new tool for the automated reduction of photometric observations. *Astronomische Nachrichten*, 340 (1-3), 68–70. <https://doi.org/10.1002/asna.201913562>
27. Khlamov, S., Vlasenko, V., Savanevych, V., Briukhovetskiy, O., Trunova, T., Chelombitko, V., Tabakova, I. (2022). Development of computational method for matched filtration with analytical profile of the blurred digital image. *Eastern-European Journal of Enterprise Technologies*, 5 (4 (119)), 24–32. <https://doi.org/10.15587/1729-4061.2022.265309>
28. Khlamov, S., Savanevych, V., Vlasenko, V., Briukhovetskiy, O., Trunova, T., Levykin, I. et al. (2023). Development of the matched filtration of a blurred digital image using its typical form. *Eastern-European Journal of Enterprise Technologies*, 1(9 (121)), 62–71. <https://doi.org/10.15587/1729-4061.2023.273674>
29. Burger, W., Burge, M. J. (2022). *Digital Image Processing. An Algorithmic Introduction*. Springer Cham, 945. <https://doi.org/10.1007/978-3-031-05744-1>
30. Bodyanskiy, Y., Popov, S., Brodetskiy, F., Chala, O. (2022). Adaptive Least-Squares Support Vector Machine and its Combined Learning-Selflearning in Image Recognition Task. 2022 IEEE 17th International Conference on Computer Sciences and Information Technologies (CSIT). <https://doi.org/10.1109/csit56902.2022.10000518>
31. Troianskiy, V., Kashuba, V., Bazyey, O., Okhotko, H., Savanevych, V., Khlamov, S., Briukhovetskiy, A. (2023). First reported observation of asteroids 2017 AB8, 2017 QX33, and 2017 RV12. *Contributions of the Astronomical Observatory Skalnaté Pleso*, 53 (2). <https://doi.org/10.31577/caosp.2023.53.2.5>
32. Li, T., DePoy, D. L., Marshall, J. L., Nagasawa, D. Q., Carona, D. W., Boada, S. (2014). Monitoring the atmospheric throughput at Cerro Tololo Inter-American Observatory with aTmCam. *Ground-Based and Airborne Instrumentation for Astronomy V*. <https://doi.org/10.1117/12.2055167>
33. Luo, X., Gu, S., Xiang, Y., Wang, X., Yeung, B., Ng, E. et al. (2022). Active longitudes and starspot evolution of the young rapidly rotating star USNO-B1.0 1388–0463685 discovered in the Yunnan–Hong Kong survey. *Monthly Notices of the Royal Astronomical Society*, 514 (1), 1511–1521. <https://doi.org/10.1093/mnras/stac1406>
34. Lemur software. CoLiTec. Available at: <https://colitec.space/>
35. Khlamov, S., Savanevych, V., Briukhovetskiy, O., Tabakova, I., Trunova, T. (2022). Data Mining of the Astronomical Images by the CoLiTec Software. *CEUR Workshop Proceedings*, 3171, 1043–1055. Available at: <https://ceur-ws.org/Vol-3171/paper75.pdf>
36. Dougherty, E. R. (2020). *Digital Image Processing Methods*. CRC Press, 504. <https://doi.org/10.1201/9781003067054>
37. Gonzalez, R., Woods, R. (2018). *Digital image processing*. Pearson. Available at: <https://dl.icdst.org/pdfs/files4/01c56e081202b62bd7d3b4f8545775fb.pdf>
38. Shvedun, V. O., Khlamov, S. V. (2016). Statistical modeling for determination of perspective number of advertising legislation violations. *Actual Problems of Economics*, 184 (10), 389–396.
39. Perova, I., Brazhnykova, Y., Miroshnychenko, N., Bodyanskiy, Y. (2020). Information Technology for Medical Data Stream Mining. 2020 IEEE 15th International Conference on Advanced Trends in Radioelectronics, Telecommunications and Computer Engineering (TCSET). <https://doi.org/10.1109/tcset49122.2020.235399>
40. Steger, C., Ulrich, M., Wiedemann, C. (2018). *Machine vision algorithms and applications*. John Wiley & Sons, 516.
41. Khlamov, S., Tabakova, I., Trunova, T., Deineko, Z. (2022). Machine Vision for Astronomical Images Using the Canny Edge Detector. *CEUR Workshop Proceedings*, 3384, 1–10.
42. Ruban, I., Martovytskiy, V., Lukova-Chuiko, N. (2016). Designing a monitoring model for cluster super-computers. *Eastern-European Journal of Enterprise Technologies*, 6 (2 (84)), 32–37. <https://doi.org/10.15587/1729-4061.2016.85433>
43. Buslov, P., Shvedun, V., Streltsov, V. (2018). Modern Tendencies of Data Protection in the Corporate Systems of Information Consolidation. 2018 International Scientific-Practical Conference Problems of Infocommunications. Science and Technology (PIC S&T). <https://doi.org/10.1109/infocommst.2018.8632089>
44. Cavuoti, S., Brescia, M., Longo, G. (2012). Data mining and knowledge discovery resources for astronomy in the web 2.0 age. *Software and Cyberinfrastructure for Astronomy II*. <https://doi.org/10.1117/12.925321>
45. Petrychenko, A., Levykin, I., Iuriev, I. (2021). Improving a method for selecting information technology services. *Eastern-European Journal of Enterprise Technologies*, 2 (2 (110)), 32–43. <https://doi.org/10.15587/1729-4061.2021.229983>
46. Grebennik, I., Chorna, O., Urniaieva, I. (2022). Distribution of Permutations with Different Cyclic Structure in Mathematical Models of Transportation Problems. 2022 12th International Conference on Advanced Computer Information Technologies (ACIT). <https://doi.org/10.1109/acit54803.2022.9913183>
47. Baranova, V., Zeleniy, O., Deineko, Z., Bielcheva, G., Lyashenko, V. (2019). Wavelet Coherence as a Tool for Studying of Economic Dynamics in Infocommunication Systems. 2019 IEEE International Scientific-Practical Conference Problems of Infocommunications, Science and Technology (PIC S&T). <https://doi.org/10.1109/picst47496.2019.9061301>
48. Dombrovska, S., Shvedun, V., Streltsov, V., Husarov, K. (2018). The prospects of integration of the advertising market of Ukraine into the global advertising business. *Problems and Perspectives in Management*, 16 (2), 321–330. [https://doi.org/10.21511/ppm.16\(2\).2018.29](https://doi.org/10.21511/ppm.16(2).2018.29)